Nanoscale

PAPER

View Article Online
View Journal | View Issue

Cite this: *Nanoscale*, 2017, **9**, 13209

Quintuple super bonding between the superatoms of metallic clusters†

Haiyan Wang[a] and Longjiu Cheng *[a,b]

Received 2nd May 2017,
Accepted 10th August 2017

DOI: 10.1039/c7nr03114a

rsc.li/nanoscale

The synthesis of a stable compound with Cr–Cr quintuple bonding (σ, 2π, 2δ) opened the door to a new field of chemistry (T. Nguyen, A. D. Sutton, M. Brynda, J. C. Fettinger, G. J. Long and P. P. Power, *Science*, 2005, **310**, 844). Looking back to the mass experiments on sodium clusters (W. D. Knight, K. Clemenger, W. A. de Heer, W. A. Saunders, M. Y. Chou and M. L. Cohen, *Phys. Rev. Lett.*, 1984, **52**, 2141), this work tells some new stories about the experimentally viewed magic numbers 26e and 30e. By unbiased global search, the 26e $Li_{20}Mg_3$ cluster has a perfect double-icosahedral motif with a large HOMO–LUMO energy gap (1.44 eV). We theoretically found that each icosahedron is an independent superatom and molecule-like electronic shell-closure is achieved *via* quintuple super bonding between two superatoms: $[8e](1D2S)^5$–$(1D2S)^5[8e]$. Similar quintuple bonding also exists in the 30e double-icosahedral $Li_{18}Mg_3Al_2$ cluster: $[8e](1D2S)^7$–$(1D2S)^7[8e]$. The 26e/30e quintuple bonding was verified by the beautiful analogies in molecular orbital diagrams and chemical bonding patterns with V_2/Re_2 molecules. Such a quintuple super bonding makes a bridge between the jellium model and chemical bonding, which further expands the community of chemical bonds.

Introduction

Bond order is a fundamental concept in chemistry. The maximum bond order can only be three (σ, 2π) for the p-block elements, and it was long believed that this is the highest bond order that can be achieved in a stable molecule. In 1964, Cotton *et al.* reported the synthesis of a salt containing the $[Re_2Cl_8]^{2-}$ ion, which revealed a quadruple bond (σ, 2π, δ) between the Re atoms.[1] In 2005, Nguyen *et al.* successfully synthesized a stable compound with quintuple bonding (σ, 2π, 2δ) between two Cr atoms.[2] These findings broke the limit of bond order three and opened the door to a new field of chemistry, which has attracted great interest both experimentally and theoretically in the study of metal–metal bonding in which the maximum bond order reaches four to six.[3–11]

In metals, due to the large number of coordination atoms and the small number of valence electrons in each metal atom, there is usually no localized metal–metal bond, and the valence electrons are freely delocalized in the whole space. The situation in finite-size metallic clusters is also similar, and is usually described using a jellium model,[12,13] which assumes a uniform background of positive charge of the cluster's atomic nuclei and the innermost electrons, in which valence electrons move freely and are subjected to an external potential. Thereby, the whole cluster can be viewed as a superatom (SA). Based on the definition, the superatomic nucleus is the sum of metal cations, which is in three-dimension different from the zero-dimension atomic nucleus. Thus, the appropriate aufbau rule of electronic shells in SAs is also different from that in atoms. For spherical sodium clusters, the appropriate aufbau rule is $|1S^2|1P^6|1D^{10}2S^2|1F^{14}2P^6|$... (capital letters are used to distinguish from that of atomic shells), associated with magic numbers 2, 8, 20, 40..., in good agreement with the peaks viewed in mass experiments.[12,13] The model of SA has achieved great success in understanding the electronic stability and chemical behaviour of experimentally produced metal clusters,[14–22] and opened the new door in chemistry and materials science expanding the periodic table of elements from two- to three-dimensions.[23–25]

For a long time, in the study of SA–SA or SA–atom interactions, only conventional atom–atom bonds have been considered, where SA shells are independent and delocalized only in the volume of each SA. In 2013, Cheng and Yang[26] proposed the super valence bond (SVB) model for real SA–SA bonding. In the SVB model, a prolate cluster is divided into two spherical blocks sharing the atomic nuclei at the border, of which each block is viewed as a SA following the electronic shells in the jellium model, and molecule-like electronic shell-closure is

[a]*Department of Chemistry, Anhui University, Hefei, Anhui 230601, P. R. China. E-mail: clj@ustc.edu*
[b]*AnHui Province Key Laboratory of Chemistry for Inorganic/Organic Hybrid Functionalized Materials, Hefei, Anhui 230601, P. R. China*

†Electronic supplementary information (ESI) available: Comparison of the MO orbitals of the $Li_{18}Mg_3Al_2$ cluster and the Re_2 molecule, and the *xyz* coordinates of the structures. See DOI: 10.1039/c7nr03114a

achieved by sharing electron pairs between two SAs. Based on the SVB model, the Li_{10} and Li_{14} clusters viewed as small peaks in the mass experiment are exact analogous of simple molecules N_2 and F_2, respectively, in electronic states and bonding patterns.[26] Similar SA–SA or SA–atom bonding was also found in bare or ligand-protected Au nanoclusters.[27–30]

Compared to the electronic shells in atoms, the D and F orbitals appear earlier in SAs. Moreover, the gaps between different orbitals of a SA are much smaller than that in an atom, which is beneficial for orbital hybridizations. Thus, similar SA–SA quintuple bonds should also exist as in transition metals. Looking back again to the pioneering mass spectra of alkali metal clusters,[12] it is found that the peaks at 26e and 30e viewed in the experiments do not follow the magic numbers in the jellium model (see Fig. S1 in the ESI†). Interestingly, we found perfect analogies between the 26e/30e metallic clusters and diatomic molecules V_2/Re_2 in molecular orbital (MO) diagrams and chemical bonding patterns, where D–D quintuple super bonding exists for shell closure.

Results and discussion

Firstly, we try to uncover the story about the magic number 26e viewed in the mass spectra of alkali metal clusters. Lithium is the first alkali metal, which can be considered as an ideal prototype for simple metals. We performed an unbiased global search on the potential energy surface of the Li_{26} cluster using the density functional theory (DFT)-based genetic algorithm implemented in our group. As shown in Fig. 1a, the first three lowest-energy isomers (**A1**–**A3**) of the Li_{26} cluster have a face-fusion bi-icosahedron patched by three atoms on the waist, and the energy differs slightly with different patch positions. However, the high-symmetry T_d isomer (**A4**) is 0.37 eV higher in energy than **A1**, despite its closed shell in geometry. **A1** has a fairly large HOMO–LUMO energy gap (E_{HL} = 1.17 eV), and the double-icosahedral feature of **A1** indicates that it may have molecule-like electron shells similar to those in $Au_{38}(SR)_{24}$ clusters,[27] that is the whole cluster is a molecule bonded by two SAs. The close-shell bi-icosahedral cluster has 23 atoms and **A1** is open-shell in geometry due to the three patched atoms. To verify the SA–SA bonding feature more clearly and easily, we built a D_{3h} $Li_{20}Mg_3$ cluster (**B1**, Fig. 1b) by replacing the central Li_6 in **A1** with Mg_3, which also has 26 valance electrons. **B1** is closed-shell in geometry and has a larger HOMO–LUMO energy gap (1.44 eV) than **A1**. Moreover, **B1** is verified to be the global minimum structure by unbiased global search. The second isomer (**B2**) is more spherical but is 0.35 eV higher in energy than **B1**.

In our opinion, the double-icosahedral **B1** should be viewed as a union of two icosahedral SAs. Each icosahedron has 13 valence electrons, which is open shell based on the jellium model: $[1S^21P^6](1D2S)^5$. However, molecule-like electronic shell-closure can be achieved *via* five-fold superbonding between two icosahedral SAs: $[8e](1D2S)^5$–$(1D2S)^5[8e]$. To verify this surmise, Fig. 2a shows the canonical MO diagrams of the

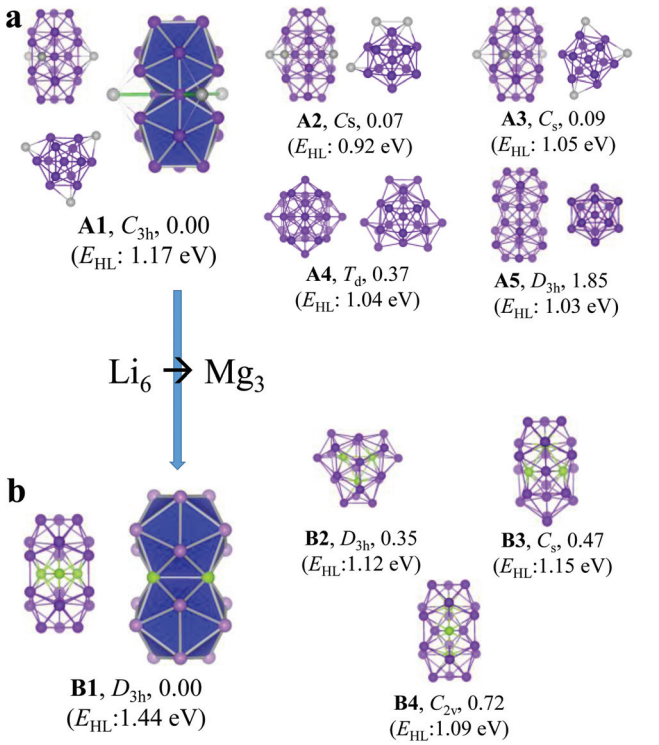

Fig. 1 Optimized low-energy isomers of (a) Li_{26} and (b) $Li_{20}Mg_3$ clusters at the PBE0/6-311+G* level of theory. Labeled are point groups, relative energies in eV, and HOMO–LUMO energy gaps. Pink and green circles represent Li and Mg atoms, respectively. Both side and top views are given for Li_{26} clusters and the patched atoms are shown in gray color.

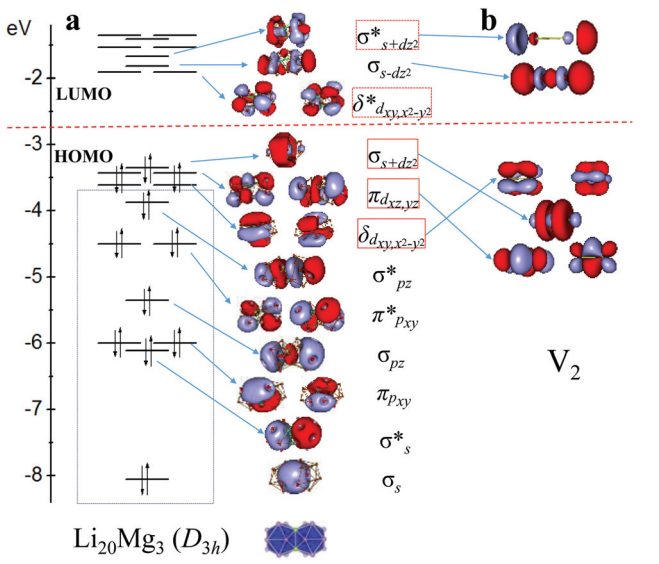

Fig. 2 Comparison of the Kohn–Sham MO diagrams of (a) the $Li_{20}Mg_3$ cluster (PBE0/6-31G*) and (b) the V_2 molecule (PBE0/def2-TZVP).

valance shells of **B1**. As expected, the first 8 MOs can be viewed as 4 bonding orbitals (σ_s, $2\pi_{px,py}$, σ_{pz}) and 4 anti-bonding orbitals (σ^*_s, $2\pi^*_{px,py}$, σ^*_{pz}), which correspond to 4 super lone pair (LP) orbitals in the inner core of each SA

($1S^2 1P^6$). Then, the five occupied frontier orbitals are two double-degenerate δ-bonding orbitals of $1D_{xy,x^2-y^2}$, two double-degenerate π-bonding orbitals of $1D_{yz,zx}$, and one σ-bonding orbital of 2S + D_{z^2}. The LUMOs are two double-degenerate δ^*_{dxy,dx^2-y^2} anti-bonding orbitals, and then one σ_{s-dz^2} bonding orbital and one $\sigma^*_{s+dz^2}$ anti-bonding orbital. There is a fairly large HOMO–LUMO gap from σ_{s+dz^2} to δ^*_{dxy,dx^2-y^2} (1.44 eV). As shown in Fig. 2b, the bonding feature in **B1** is analogous to that in the V_2 molecule from canonical MOs: $[Ar](3d4s)^5$–$(3d4s)^5[Ar]$. The occupied valence MOs of V_2 are five bonding orbitals ($2\pi_{dyz,dzx}$, σ_{s+dz^2}, $2\delta_{dxy,dx^2-y^2}$). The LUMO is the σ_{s-dz^2} bonding orbital, and then is the $\sigma^*_{s+dz^2}$ anti-bonding orbital. There are good analogies in orbital shapes between the MOs of **B1** and V_2, and the difference is the order of the energy levels of MOs. Two SAs in **B1** are relatively closer to each other, which decreases the energy level of the δ-bonding orbital and increases the energy level of the σ-bonding orbital.

To further confirm the existence of quintuple bonding in **B1**, we investigated its chemical bonding patterns by using the adaptive natural density partitioning (AdNDP)[31] method, which is a powerful tool for deciphering the multicenter bonding in molecules and clusters with delocalized electrons. As shown in Fig. 3a, AdNDP chemical bonding analysis reveals four 13c–2e super LPs in each SA ($1S^2 1P^6$) and five 23c–2e quintuple SA–SA bonds (σ, 2π, 2δ). Fig. 3b also shows the AdNDP chemical bonding of V_2, and one can see that there are very beautiful analogies between the shape of the quintuple bonds in **B1** and V_2. The high occupancy numbers (ONs ≥ 1.99|*e*|) indicate high reliability of the AdNDP results, except for the super P_z lone pair (ON = 1.89|*e*|), which may be due to the hybridization of $1P_z$, $1D_{z^2}$ and 2S orbitals along the *z*-axis.

It should be mentioned that there is also a quintuple super bond in the isomer **B4**. There is a high electron density at the border of two SAs due to the quintuple super bond. **B1** has more positive charges (three Mg^{2+}) at the border, so it is more stable than **B4**.

Next, we will uncover the story about the magic number 30e viewed in the pioneering mass spectra. To obtain such a 30e cluster, we simply replaced the two Li atoms at the centers of the icosahedra by Al atoms (**C1**, $Li_{18}Mg_3Al_2$) to add four valence electrons, instead of unbiased global search. After structural relaxation and frequency check at the PBE0/6-311+G* level of theory, **C1** is verified to be a true local minimum structure, which maintains the D_{3h} symmetry and has a fairly large HOMO–LUMO energy gap (0.95 eV).

The 30e double-icosahedral **C1** may also be viewed as a super diatomic molecule: $[8e](1D2S)^7$–$(1D2S)^7[8e]$, where $1S^2 1P^6$ [8e] can be viewed as the inner core. As shown in Fig. 4a, AdNDP chemical bonding analysis is also performed on **C1** to study its electronic structure. As expected, AdNDP analysis viewed four 13c–2e super LPs ($1S^2 1P^6$) delocalized in each SA with a very high occupancy number (ON ≥ 1.99|*e*|). There is another 13c–2e super LP in each SA with ON = 1.77|*e*|, which seems to be a hybrid orbital of 2S and $1D_{z^2}$ (2S + $1D_{z^2}$). Similarly, the remaining 10 electrons form 23c–2e quintuple super bonds (σ, 2π, 2δ) between two SAs with ON ≥ 1.98|*e*|. The main component of the super σ bond in **C1** is 2S–$1D_{z^2}$, and thus it is quite different in shape from that in **B1** (2S + $1D_{z^2}$). As shown in Fig. 4b, such a quintuple super bond in **C1** is also a nice analogue of the Re_2 molecule: $[Xe](5d6s)^7$–$(5d6s)^7[Xe]$. There are perfect analogies between the AdNDP chemical bonding of **C1** and Re_2. Such a quintuple super bond can also be verified by the MO diagrams (see Fig. S2 in the ESI†).

The SA shells in the jellium model of metal clusters are actually MOs, and the original definition of the superatoms of metal clusters is due to the similarity between the MOs in the jellium model and the atomic shells. However, in the 26e and 30e cases, MOs in the jellium model mimic the orbitals of a molecule instead of an atom, so we can take the metal cluster

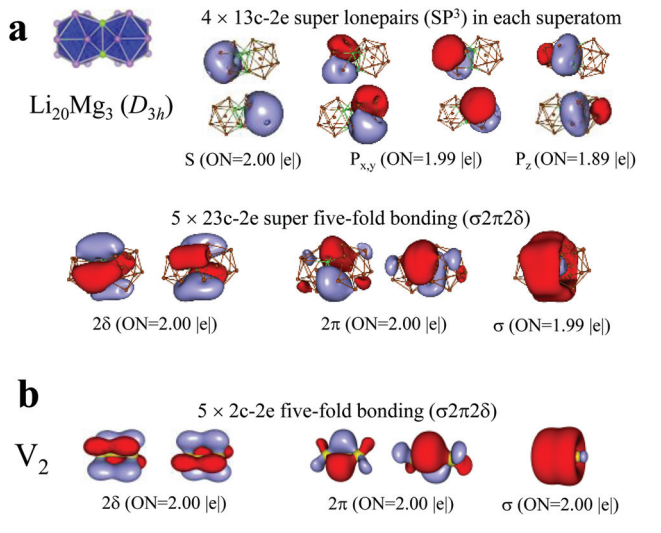

Fig. 3 Structures and AdNDP localized natural bonding orbitals of (a) the $Li_{20}Mg_3$ cluster (PBE0/6-31G*) and (b) the V_2 molecule (PBE0/def2-TZVP). ON gives the occupancy numbers.

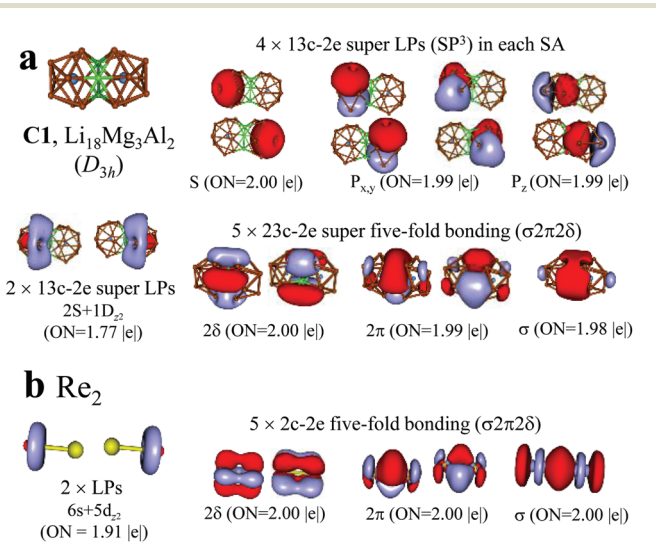

Fig. 4 AdNDP localized natural bonding orbitals of (a) the $Li_{18}Mg_3Al_2$ cluster (PBE0/6-31G*) and (b) the Re_2 molecule (PBE0/def2-TZVP).

as a superatomic-molecule. In molecules, atoms are separate and the border between atoms is obvious. However, in the superatomic-molecule model, the metallic cluster is divided into different SAs empirically, and the border between SAs depends on the division. In the two double-icosahedral $Li_{20}Mg_3$ and $Li_{18}Mg_3Al_2$ clusters, the border is the Mg_3 triangular face shared by two icosahedra, *i.e.*, the three Mg atoms are shared by two SAs. The valence electrons are freely delocalized over the whole cluster volume in the jellium model. In the superatomic-molecule model, inner-core electrons (such as 8e) are delocalized over only the volume of individual SAs, and the bonding electrons are delocalized over the volume of two SAs to achieve a molecule-like electronic shell-closure. Thus, we just expanded the concept from a SA to a superatomic molecule *via* the model of SA–SA bonding, whose shell order of the SA also follows the jellium model.

Conclusions

In summary, looking back to the pioneering mass experiments on sodium clusters in 1984, we found some new stories about the magic numbers 26e and 30e that dissatisfy the rule in the jellium model. Using unbiased global search, we found that the Li_{26} cluster has a double-icosahedral global minimum structure with three patched atoms. By unbiased global search, it is also verified that the 26e $Li_{20}Mg_3$ cluster has a perfect D_{3h} double-icosahedral global minimum structure with a large HOMO–LUMO energy gap (1.44 eV). From the molecular orbital diagrams and chemical bonding patterns, it is found that each icosahedron in the $Li_{20}Mg_3$ cluster is an independent superatom and molecule-like electronic shell-closure is achieved *via* quintuple bonding between two superatoms: $[8e](1D2S)^5$–$(1D2S)^5[8e]$. Similar quintuple bonding also exists in the 30e double-icosahedral $Li_{18}Mg_3Al_2$ cluster: $[8e](1D2S)^7$–$(1D2S)^7[8e]$. The analogies of quintuple super bonding in the 26e/30e clusters and quintuple bonding in V_2/Re_2 molecules are very beautiful and straightforward.

Chemical bonding is the basic language of chemistry, which is the basis for the building blocks of molecules and materials. However, metallic clusters cannot be described using the language of chemical bonding, and the jellium model is the common language in this field. The quintuple super bonding viewed in the $Li_{20}Mg_3$ and $Li_{18}Mg_3Al_2$ nanoalloy clusters may act as a hybrid language, which makes a bridge between these two common languages – chemical bonding and jellium model. It can be expected that a similar mechanism may also exist in the solid, and the electronic structures of certain bulk alloys may be explained using the hybrid language of SA–SA super bonding.

Computational method

Computational details

The structures are located by unbiased global search of the potential energy surface using a genetic algorithm at the DFT level of theory. To guarantee the performance of global search, over 5000 local minimum structures are sampled for each case. DFT calculations are carried out using the Gaussian 09 package,[32] using the PBE0 functional[33] with the 6-311+G* basis set for Li, Mg, and Al, and the relativistic effective core potential basis set (def2-TZVP) for V and Re. All the structures given in this paper are true local minimum verified by frequency check. The HOMO–LUMO energy gaps are calculated at the PBE0/6-311+G* level of theory, while MO diagrams and AdNDP chemical bonding analysis are carried out at the PBE0/63-1G*/def2-TZVP level of theory using the optimized geometries. MO visualization is performed using MOLEKEL 5.4 software.[34]

Conflicts of interest

There are no conflicts to declare.

Acknowledgements

This work is financed by the National Natural Science Foundation of China (21573001) and by the Foundation of Distinguished Young Scientists of Anhui Province.

Notes and references

1 F. Cotton, N. Curtis, C. Harris, B. Johnson, S. Lippard, J. Mague, W. Robinson and J. Wood, *Science*, 1964, **145**, 1305–1307.
2 T. Nguyen, A. D. Sutton, M. Brynda, J. C. Fettinger, G. J. Long and P. P. Power, *Science*, 2005, **310**, 844–847.
3 L. Gagliardi and B. O. Roos, *Nature*, 2005, **433**, 848–851.
4 M. Brynda, L. Gagliardi, P. O. Widmark, P. P. Power and B. O. Roos, *Angew. Chem., Int. Ed.*, 2006, **45**, 3804–3807.
5 U. Radius and F. Breher, *Angew. Chem., Int. Ed.*, 2006, **45**, 3006–3010.
6 G. Merino, K. J. Donald, J. S. D'Acchioli and R. Hoffmann, *J. Am. Chem. Soc.*, 2007, **129**, 15295–15302.
7 B. O. Roos, A. C. Borin and L. Gagliardi, *Angew. Chem., Int. Ed.*, 2007, **46**, 1469–1472.
8 F. R. Wagner, A. Noor and R. Kempe, *Nat. Chem.*, 2009, **1**, 529–536.
9 R. J. Eisenhart, L. J. Clouston and C. C. Lu, *Acc. Chem. Res.*, 2015, **48**, 2885–2894.
10 D.-Y. Lu, P. P. Y. Chen, T.-S. Kuo and Y.-C. Tsai, *Angew. Chem., Int. Ed.*, 2015, **54**, 9106–9110.
11 A. Noor, G. Glatz, R. Mueller, M. Kaupp, S. Demeshko and R. Kempe, *Nat. Chem.*, 2009, **1**, 322–325.
12 W. D. Knight, K. Clemenger, W. A. de Heer, W. A. Saunders, M. Y. Chou and M. L. Cohen, *Phys. Rev. Lett.*, 1984, **52**, 2141–2143.
13 W. A. de Heer, *Rev. Mod. Phys.*, 1993, **65**, 611.
14 R. Leuchtner, A. Harms and A. Castleman Jr., *J. Chem. Phys.*, 1989, **91**, 2753.
15 K. E. Schriver, J. L. Persson, E. C. Honea and R. L. Whetten, *Phys. Rev. Lett.*, 1990, **64**, 2539–2542.

16 D. E. Bergeron, A. W. Castleman, T. Morisato and S. N. Khanna, *Science*, 2004, **304**, 84–87.
17 D. E. Bergeron, P. J. Roach, A. W. Castleman, N. O. Jones and S. N. Khanna, *Science*, 2005, **307**, 231–235.
18 A. C. Reber, S. N. Khanna and A. W. Castleman Jr., *J. Am. Chem. Soc.*, 2007, **129**, 10189–10194.
19 M. Walter, J. Akola, O. Lopez-Acevedo, P. D. Jadzinsky, G. Calero, C. J. Ackerson, R. L. Whetten, H. Gronbeck and H. Hakkinen, *Proc. Natl. Acad. Sci. U. S. A.*, 2008, **105**, 9157–9162.
20 L. Cheng, Y. Yuan, X. Zhang and J. Yang, *Angew. Chem., Int. Ed.*, 2013, **52**, 9035–9039.
21 Z. Luo and A. W. Castleman, *Acc. Chem. Res.*, 2014, **47**, 2931–2940.
22 P. Jena, *J. Phys. Chem. Lett.*, 2015, **6**, 1549–1552.
23 A. W. Castleman Jr. and S. N. Khanna, *J. Phys. Chem. C*, 2009, **113**, 2664–2675.
24 S. A. Claridge, A. W. Castleman, S. N. Khanna, C. B. Murray, A. Sen and P. S. Weiss, *ACS Nano*, 2009, **3**, 244–255.
25 P. Jena, *J. Phys. Chem. Lett.*, 2013, **4**, 1432–1442.
26 L. Cheng and J. Yang, *J. Chem. Phys.*, 2013, **138**, 141101.
27 L. J. Cheng, C. D. Ren, X. Z. Zhang and J. L. Yang, *Nanoscale*, 2013, **5**, 1475–1478.
28 Y. Yuan, L. Cheng and J. Yang, *J. Phys. Chem. C*, 2013, **117**, 13276–13282.
29 L. J. Cheng, X. Z. Zhang, B. K. Jin and J. L. Yang, *Nanoscale*, 2014, **6**, 12440–12444.
30 L. Yan, L. Cheng and J. Yang, *J. Phys. Chem. C*, 2015, **119**, 23274–23278.
31 D. Y. Zubarev and A. I. Boldyrev, *Phys. Chem. Chem. Phys.*, 2008, **10**, 5207–5217.
32 M. Frisch, G. Trucks, H. Schlegel, G. Scuseria, M. Robb, J. Cheeseman, G. Scalmani, V. Barone, B. Mennucci and G. Petersson, Gaussian Inc., Wallingford, CT, 2010.
33 A. Carlo and V. Barone, *J. Chem. Phys.*, 1999, **110**, 6158–6170.
34 U. Varetto, MOLEKEL 5.4, Swiss National Supercomputing Centre, Manno, Switzerland, 2009.